DIVISION OF ANTIVIRALS, CDER/OND/OID
CLINICAL VIROLOGY REVIEW
EUA: 000105 **SDNs:** 186, 206, 232, 235 **SNs:** 180, 200, 224, 228 **DATE REVIEWED:** 9/7/2022

Reviewer: Jonathan Rawson, Ph.D.
Dates Submitted: 7/29/2022, 8/24/2022, 9/19/2022, 9/22/2022
Dates Received: 7/29/2022, 8/24/2022, 9/19/2022, 9/22/2022
Dates Assigned: 8/1/2022, 8/24/2022, 9/20/2022, 9/23/2022

Sponsor: Pfizer Global Regulatory Affairs
235 East 42nd Street
New York, NY 10017-5755
Karen Baker, Director, Pfizer Global Regulatory Affairs

Product Names: nirmatrelvir (PF-07321332, PAXLOVID™; coadministered with ritonavir)
Chemical Name: 1R,2S,5S)-N-((1S)-1-Cyano-2-((3S)-2-oxopyrrolidin-3-yl)ethyl)-3-((2S)-3,3-dimethyl-2-(2,2,2-trifluoroacetamido)butanoyl)-6,6-dimethyl-3-azabicyclo[3.1.0]hexane-2-carboxamide

Structure:

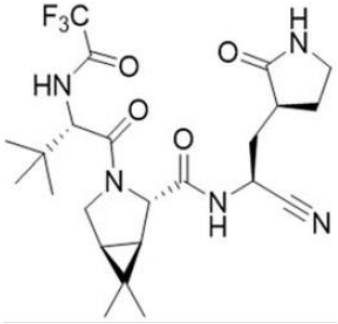

NIRMATRELVIR (PF-07321332)

Molecular Formula: $C_{23}H_{32}F_3N_5O_4$
Molecular Weight: 499.54 daltons
Drug Category: Antiviral
Indication: Treatment of mild-to-moderate COVID-19
Dosage Form/Route of Administration: nirmatrelvir 150 mg tablet, coadministered with ritonavir 100 mg tablet / oral
Supporting Documents: IND 153517
Abbreviations: BID, twice daily; CoV, coronavirus; CPE, cytopathic effect; MA, mouse-adapted; MHV, mouse hepatitis virus; MOI, multiplicity of infection; M^{pro}, main protease; NIR/r, nirmatrelvir/ritonavir; P-gp, P-glycoprotein; PK, pharmacokinetics; qRT-PCR, quantitative reverse transcription polymerase chain reaction; SARS, severe acute respiratory syndrome; $TCID_{50}$; median tissue culture infectious dose; TMPRSS2, transmembrane protease serine 2; WT, wild-type

SUBMISSION OVERVIEW

These submissions relate to an application for Emergency Use Authorization for nirmatrelvir/ritonavir (NIR/r, PAXLOVID™, PF-07321332/r; EUA 000105 and IND 153517). NIR/r was authorized on 12/22/2021 for the treatment of mild-to-moderate COVID-19 in adults and pediatric patients (12 years of age and older weighing at least 40 kg) with positive results of direct SARS-CoV-2 viral testing, and who are at high risk for progression to severe COVID-19, including hospitalization or death. This review covers several new and updated nonclinical virology study reports and proposed revisions to section 12.4 of the PAXLOVID™ Fact Sheet for Healthcare Providers.

NONCLINICAL VIROLOGY

Activity Against SARS-CoV-2 Variants

The sponsor proposes to revise the PAXLOVID fact sheet to indicate that NIR retains activity against the SARS-CoV-2 Omicron sub-variants BA.2, BA.2.12.1, and BA.4 in cell culture. To support the proposed changes, the sponsor submitted Report 042713 (version 5.0, "In Vitro RT-qPCR-Based Efficacy of PF-07321332 Against Major SARS-CoV-2 Variants"). In this report, the activity of NIR against SARS-CoV-2 USA-WA1/2020, BA.2, BA.2.12.1, and BA.4 variants was determined in Vero E6-TMPRSS2 cells by qRT-PCR. Relative to USA-WA1/2020, the BA.2, BA.2.12.1, and BA.4 isolates contained the expected M^{pro} P132H polymorphism, but none of the isolates had any other amino acid polymorphisms in M^{pro} or any amino acid polymorphisms in M^{pro} cleavage sites. NIR activity was tested in the presence of 2,000 nM CP-100356, a P-glycoprotein (P-gp) inhibitor. Cells were infected at a multiplicity of infection (MOI) of 0.04, with compounds added at the time of infection. Cells were lysed 48 hours post-infection, and SARS-CoV-2 RNA levels were determined by qRT-PCR. NIR retained activity against the SARS-CoV-2 Omicron sub-variants BA.2, BA.2.12.1, and BA.4, with fold-changes in the EC_{50} and EC_{90} values <1 relative to USA-WA1/2020 (Table 1). Consistent with these findings, several independent groups have found that NIR retains activity against the SARS-CoV-2 Omicron sub-variants BA.2, BA.2.12.1, BA.2.75, BA.4, and BA.5 in cell culture (Bojkova et al., 2022, Ohashi et al., 2022, Saito et al., 2022, Takashita et al., 2022, Takashita et al., 2022, Takashita et al., 2022).

Table 1. Nirmatrelvir activity against SARS-CoV-2 Omicron sub-variants in Vero E6-TMPRSS2 cells (+ P-gp inhibitor).

SARS-CoV-2 Isolate	n	Geomean EC_{50} (nM) (Range)	EC_{50} Fold-Change	Geomean EC_{90} (nM) (Range)	EC_{90} Fold-Change
USA-WA1/2020	7	70 (49 – 98)	N/A	211 (123 – 478)	N/A
Omicron BA.2	5	65 (52 – 78)	0.9	132 (95 – 162)	0.6
Omicron BA.2.12.1	5	40 (34 – 44)	0.6	114 (72 – 408)	0.5
Omicron BA.4	3	39 (19 – 54)	0.6	98 (92 – 104)	0.5

Source: Adapted from Report 042713, p. 16. n, number of experiments; N/A, not applicable.

Antiviral Activity in Animal Models

The sponsor proposes to revise the PAXLOVID fact sheet to include data from a new study in mice (Report 092629, "In Vivo Efficacy of PF-07321332 as a Single Agent or in Combination with Ritonavir in BALB/c Mouse-Adapted SARS-CoV-2 Model"). In this report, the activities of NIR, ritonavir, and NIR+ritonavir were evaluated against mouse-adapted (MA) SARS-CoV-2 MA10 in BALB/c mice in two independent studies. In BALB/c mice, SARS-CoV-2 MA10 causes severe, and in some cases lethal, lung disease (Leist et al., 2020). The extent of lethality depends on the infectious dose and age of the mice. In each study, 8- to-10-week-old female mice were inoculated intranasally with 10^5 $TCID_{50}$ of SARS-CoV-2 MA10 (Fig. 1). Mice were orally treated with NIR (300 mg/kg BID), ritonavir (50 mg/kg BID), or NIR+ritonavir (300 mg/kg+50 mg/kg BID, respectively) starting at 4 hours post-infection on Day 0 and continuing to Day 3. Thus, dosing modeled prophylaxis, not treatment of symptomatic disease. Mice were euthanized on Day 4 for determination of lung virus titers, histopathology, and immunohistochemistry. Virus titers ($TCID_{50}$/mL) were determined by cytopathic effect (CPE) assay in Vero 76 cells. With this experimental design, mice were not followed for a sufficient duration to assess the impact of NIR through the full course of disease. Uninfected, untreated and infected, vehicle-treated mice were included as controls. In addition, uninfected animals (2/dose group) were treated with NIR, ritonavir, or NIR+ritonavir for pharmacokinetics (PK) studies.

Figure 1. Experimental design to test efficacy of NIR, ritonavir, and NIR+ritonavir in SARS-CoV-2 MA10-infected BALB/c mice.

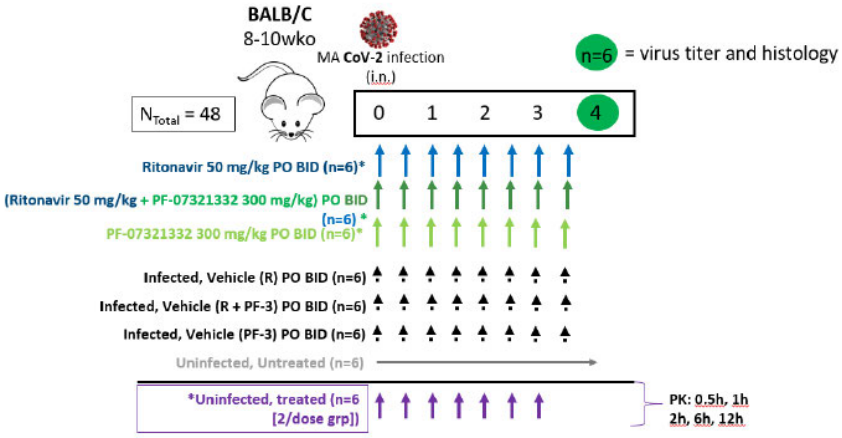

Source: Report 092629, p. 10.
BID, twice daily; h, hour; i.n., intranasal; MA, mouse-adapted; n, number of animals; PF-3/PF-07321332, nirmatrelvir; PK, pharmacokinetics; PO, dosed orally; R, ritonavir; wko, weeks old.

In vehicle-treated mice, mean lung virus titers were 5.2-5.3 $\log_{10}$ $TCID_{50}$/mL on Day 4 (Fig. 2). In ritonavir-treated mice, the mean lung virus titer was 5.4 $\log_{10}$ $TCID_{50}$/mL; thus, ritonavir alone did not have antiviral activity. In NIR-treated mice, the mean lung virus titer was 4.0 $\log_{10}$ $TCID_{50}$/mL; thus, NIR alone resulted in a 1.2 $\log_{10}$ reduction in virus titer relative to vehicle control. In mice treated with NIR+ritonavir, the mean lung virus titer was 3.7 $\log_{10}$ $TCID_{50}$/mL; thus, NIR+ritonavir resulted in a 1.6 $\log_{10}$ reduction in virus titer relative to vehicle control. The sponsor did not indicate whether the difference in lung viral titers between NIR and NIR+ritonavir was statistically significant. Results were generally consistent between the two studies.

Figure 2. Effects of NIR, ritonavir, and NIR+ritonavir on lung virus titers in SARS-CoV-2 MA10-infected mice (studies 2 and 3 combined).

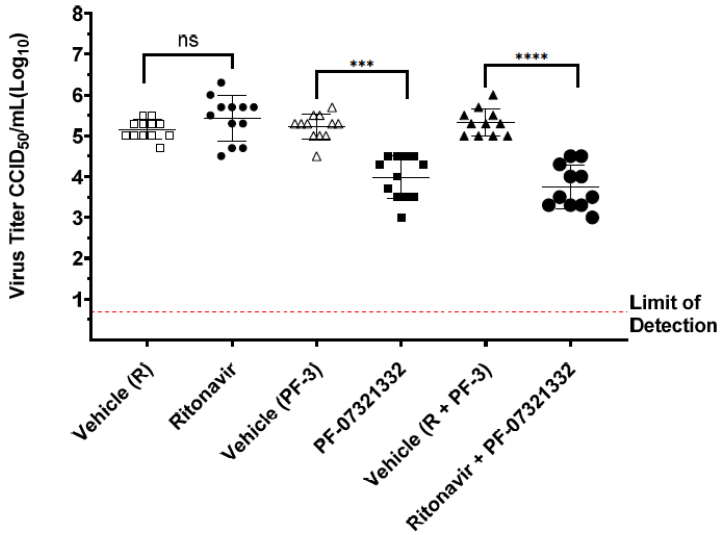

Source: Report 092629, p. 24. *** indicates p <0.001 and **** indicates p <0.0001 relative to infected vehicle-treated mice. P-values were determined by non-parametric one-way ANOVA with Kruskal-Wallis post-test.
$CCID_{50}$, median cell culture infectious dose; ns, not significant; PF-3/PF-07321332, nirmatrelvir; R, ritonavir.

In study 2, NIR alone did not reduce mean lung histopathology scores on Day 4 (Fig. 3), in contrast to results from a previous report. Ritonavir alone did not affect mean lung histopathology scores either. However, NIR+ritonavir significantly reduced the mean lung histopathology score. Histopathology findings for study 3 and immunohistochemistry results are pending and will be added to the report when available.

Figure 3. Effects of NIR, ritonavir, and NIR+ritonavir on lung histopathology scores in SARS-CoV-2 MA10-infected mice (study 2).

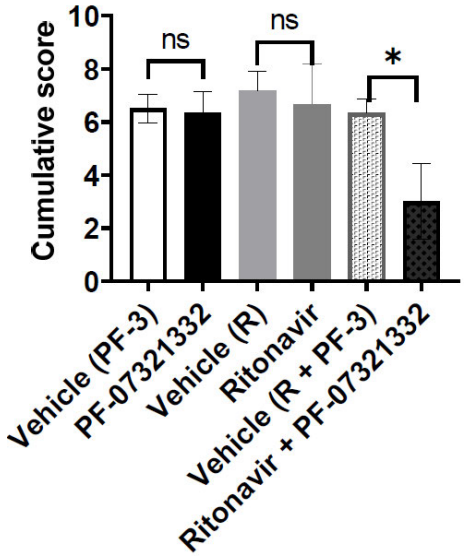

Source: Report 092629, p. 22. Lung histopathology was evaluated in a blinded fashion by an external veterinary pathologist. Four parameters were evaluated with a 5-point scoring system: perivascular inflammation, bronchial or bronchiolar epithelial degeneration or necrosis, bronchial or bronchiolar inflammation, and alveolar inflammation. The individual scores were added to calculate a cumulative pathology score. * indicates p <0.05. P-values were determined by non-parametric one-way ANOVA with Kruskal-Wallis post-test.
ns, not significant; PF-3/PF-07321332, nirmatrelvir; R, ritonavir.

PK studies were also performed using a separate group of uninfected, NIR-treated animals. In study 2, minimal unbound plasma concentrations (C_{min}) of NIR at 12 hours post-last dose were 0.9× and 8× higher (for NIR and NIR+ritonavir, respectively) than the EC_{90} value of NIR against SARS-CoV-2 in differentiated normal human bronchial epithelial cells (181 nM). In study 3, C_{min} values at 12 hr post-last dose were 2.9× and 28× higher (for NIR and NIR+ritonavir, respectively) than the EC_{90} value. These results show that ritonavir significantly increased NIR plasma exposures in BALB/c mice.

> **Comment (internal):** The sponsor has not submitted Report 092629 to EUA105. The above review is from a preliminary version of Report 092629 submitted to (b) (4) .

Resistance Development in Cell Culture
The sponsor proposes to revise the PAXLOVID fact sheet to include resistance data from three new or revised studies (Reports 065112, 113117, and 024518), which are reviewed below, and several preprints released by independent groups.

> **Comment (internal):** The sponsor has not submitted the most recent version of Report 024518 to EUA105. (b) (4) .

"In Vitro Evaluation of Selected Resistant SARS-CoV-2 Against PF-07321332 (Nirmatrelvir) in Vero E6 P-gp Knockout Cells" (Report 113117)
To identify SARS-CoV-2 M^{pro} residues associated with NIR resistance, the sponsor selected NIR-resistant SARS-CoV-2 (USA-WA1/2020) in Vero E6 P-gp knockout cells. SARS-CoV-2 was serially passaged 9 times under 5 different passaging schemes with constant or increasing NIR concentrations. In scheme #1, the NIR concentration was kept constant at 150 nM (1×EC_{50}). In schemes #2-4, the NIR concentration was progressively increased from 150 nM (1×EC_{50}) to either 1,314 nM (9×EC_{50}), 3,066 nM (21×EC_{50}), or 7,300 nM (50×EC_{50}). In scheme #5, the NIR concentration was kept constant at 370 nM (1×EC_{90}). These experiments

were conducted using a single virus stock. In addition, for schemes #1-4, the first passage was the same (i.e., the virus was split after the first passage). Cells were infected at an MOI of 0.01 for the first passage and variable MOIs thereafter. Each passage lasted 2-8 days, depending on the amount of time required to generate >50% CPE in the culture. When sufficient CPE was detected, viral supernatants were collected and used to infect cells for the next passage. Virus titers ($TCID_{50}$/mL) after each passage were determined by CPE assay in Vero E6 P-gp knockout cells. Virus was passaged in the absence of NIR as a control.

After each passage, viral RNA was extracted, and M^{pro} and M^{pro} cleavage site substitutions with frequencies ≥3% were identified by whole-genome Illumina sequencing. In schemes #1-4, which shared the first virus passage, an M^{pro} T304I substitution was identified after passage 1 (Table 2). In scheme #1, T304I gradually increased in frequency, but no other M^{pro} substitutions were observed. In schemes #2-4, T304I increased in frequency more quickly, followed by acquisition of an A173V substitution, which increased to >90% frequency in a single passage. In scheme #3, L50F (20-21%) and T135I (6%) substitutions were also observed after passages 8-9. In scheme #5, T304I was identified first, followed by T21I and S144A substitutions. L50F (6%), T135I (7%), and A191V (5%) were also observed after passages 4-5 but not after later passages. Virus that was passaged in the absence of NIR did not acquire any M^{pro} substitutions. In total, 7 distinct M^{pro} substitutions were identified: T21I, L50F, T135I, S144A, A173V, A191V, and T304I. In addition, the substitution frequencies indicate that some viruses had multiple M^{pro} substitutions, e.g., A173V+T304I, T21I+T304I, and T21I+S144A+T304I.

Table 2. Sequencing of SARS-CoV-2 passaged in the presence of NIR in Vero E6 P-gp knockout cells.

	M^{pro} Substitutions ≥3% (Frequency)				
Passage	**Scheme #1**	**Scheme #2**	**Scheme #3**	**Scheme #4**	**Scheme #5**
1	T304I (12%)	T304I (12%)	T304I (12%)	T304I (12%)	none
2	T304I (15%)	T304I (45%)	T304I (45%)	T304I (45%)	T304I (5%)
3	T304I (38%)	T304I (79%)	T304I (79%)	T304I (79%)	T304I (77%)
4	T304I (66%)	T304I (83%)	T304I (81%)	T304I (81%)	T21I (31%), L50F (6%), T135I (7%), T304I (81%)
5	T304I (68%)	T304I (74%)	A173V (12%), T304I (74%)	A173V (12%), T304I (74%)	T21I (78%), L50F (6%), S144A (43%), A191V (5%), T304I (71%)
6	T304I (73%)	A173V (5%), T304I (75%)	A173V (93%), T304I (74%)	A173V (93%), T304I (74%)	T21I (99%), S144A (94%), T304I (73%)
7	T304I (75%)	A173V (93%), T304I (76%)	A173V (93%), T304I (77%)	A173V (89%), T304I (79%)	T21I (100%), S144A (95%), T304I (77%)
8	T304I (82%)	A173V (98%), T304I (80%)	L50F (21%), T135I (6%), A173V (98%), T304I (81%)	ND	T21I (100%), S144A (100%), T304I (83%)
9	T304I (80%)	A173V (97%), T304I (80%)	L50F (20%), A173V (98%), T304I (79%)	ND	T21I (100%), S144A (100%), T304I (81%)

Source: Adapted from Report 113117, pp. 29-30.
ND, no data, as viruses could not be recovered.

To determine whether the selected viruses had reduced susceptibility to NIR, the sponsor plaque-purified a total of 88 viruses from scheme #3, passage 7 and scheme #5, passages 4-5. The viruses were screened by Sanger sequencing to identify M^{pro} substitutions. Six viruses with different M^{pro} substitutions were selected for additional analysis. These viruses were further propagated in the absence and presence of NIR to produce virus stocks and prevent reversion of M^{pro} substitutions. The virus stocks were then sequenced by whole-genome Illumina sequencing to confirm the presence of the expected substitutions. NIR activity was then determined against the 6 viruses in Vero E6 P-gp knockout cells by qRT-PCR assay. In most cases, the viruses further propagated in the presence of NIR were used for these experiments. However, the virus propagated in the absence of NIR was used for T304I.

The 6 viruses tested had M^{pro} T304I, T21I+T304I, L50F+T304I, T135I+T304I, A173V+T304I, or T21I+S144A+T304I substitutions (Table 3). For most viruses, the expected M^{pro} substitutions had frequencies ≥97%, but the L50F and T304I substitutions had frequencies of 49% and 80-82%, respectively. These results

may indicate that the plaques were not pure or that the substitutions partially reverted during propagation. Relative to the parental virus (USA-WA1/2020, historical aggregate of 23 experiments), all 6 viruses had significantly reduced susceptibility to NIR. The virus with the T304I substitution alone had 3.4-fold reduced susceptibility to NIR (based on geomean EC_{50} value). The viruses with T21I+T304I, L50F+T304I, T135I+T304I, and A173V+T304I double substitutions had 3.8- to 20.2-fold reduced susceptibility to NIR, while the virus with the T21I+S144A+T304I triple substitution had 27.8-fold reduced susceptibility to NIR. All of the viruses remained fully susceptible to remdesivir. Overall, these results indicate that most of the M^{pro} substitutions observed contributed to NIR resistance, with the possible exception of T135I.

Table 3. Activity of NIR against plaque-purified SARS-CoV-2 with M^{pro} substitutions.

		EC_{50} (nM)					EC_{90} (nM)				
M^{pro} Substitutions (Frequency)	**n**	**Geomean**	**95% CI Low Bound**	**95% CI High Bound**	**Fold-Change**	**p-value**	**Geomean**	**95% CI Low Bound**	**95% CI High Bound**	**Fold-Change**	**p-value**
none (control)	23	34.8	25.7	47.0	N/A	N/A	154	118	200	N/A	N/A
T304I (82%)	3	118	24.2	574	3.4	0.02	420	143	1,232	2.7	0.02
T21I (100%), T304I (81%)	3	275	136	554	7.9	<0.001	568	279	1,159	3.7	0.002
L50F (49%), T304I (80%)	4	205	72.4	582	5.9	<0.001	783	496	1,236	5.1	<0.001
T135I (100%), T304I (80%)	4	134	62.0	288	3.8	0.002	353	153	814	2.3	0.04
A173V (97%), T304I (82%)	3	702	150	3,287	20.2	<0.001	1,631	512	5,190	10.6	<0.001
T21I (100%), S144A (100%), T304I (82%)	4	967	438	2,136	27.8	<0.001	2,548	1,517	4,280	16.6	<0.001

Source: Adapted from Report 113117, pp. 32-33. P-values were determined by one-way ANOVA with Dunnett's post-test to compare EC_{50} values of each virus to the control virus (WA1/2020).
CI, confidence interval; n, number of experiments; N/A, not applicable.

Of the 7 distinct M^{pro} substitutions observed (T21I, L50F, T135I, S144A, A173V, A191V, and T304I), 6/7 (all except T135I) have been associated with NIR resistance in cell culture, usually in combination with other M^{pro} substitutions, by independent groups (Iketani et al., 2022; Jochmans et al., 2022; Zhou et al., 2022). In addition, the T21I+T304I, L50F+T304I, A173V+T304I, and T21I+S144A+T304I double or triple substitutions have all been associated with NIR resistance in other studies, although other M^{pro} substitutions were present as well in some cases. These findings further confirm the association of these substitutions (with the possible exception of T135I) with SARS-CoV-2 resistance to NIR in cell culture. Notably, the T304I substitution is located near the C-terminus of M^{pro}, which overlaps the nsp5/nsp6 M^{pro} cleavage site. T304I is located in the P3 position of the cleavage site and may affect binding of the nsp5/nsp6 cleavage site or M^{pro} autocleavage (Iketani et al., 2022).

These studies had several limitations. The findings were not confirmed with biochemical assays and recombinant viruses. The sponsor did not indicate whether any of the selected viruses had substitutions in any M^{pro} cleavage sites (besides the M^{pro} T304I substitution). Replication kinetics in the absence of NIR were not determined. Alternative resistance pathways may have been missed, as a single virus stock was used to initiate the infections, and the first passage was shared for 4/5 passaging schemes. No data were provided regarding the structural or mechanistic basis of resistance.

"Evaluation of In Vitro Selected Resistant SARS-CoV-2 Against PF-07321332 (Nirmatrelvir) in A549-ACE2 Cells" (Report 065112)

The sponsor also selected NIR-resistant SARS-CoV-2 (USA-WA1/2020) in A549-ACE2 cells. The activity of NIR against SARS-CoV-2 WA1/2020 in A549-ACE2 cells was first determined by virus yield reduction assay. A549-ACE2 cells were infected in the presence of NIR for 2 days, followed by collection of supernatants and virus titration in Vero E6 cells by plaque assay. NIR had an EC_{50} value of ~50 nM in this assay. SARS-CoV-2

was serially passaged 7 times with NIR concentrations increasing from 300 nM (6×EC_{50}) to 2,500 nM (50×EC_{50}). These experiments were conducted using a single virus stock, which was presumably the same stock used in the other selection study. Cells were infected at an MOI of 0.1 for passages 1-2, 0.01 for passage 3, and 0.001 for passages 4-7. Each passage lasted 3-6 days. After each passage, virus titers (pfu/mL) were determined by plaque assay in Vero E6 cells. In addition, viral RNA was extracted after each passage, and M^{pro} and M^{pro} cleavage site substitutions were identified by whole-genome Illumina sequencing.

After passage 3, an M^{pro} A173V substitution was detected at a high frequency (96%, Table 4). The A173V substitution remained predominant through passage 7, and no other M^{pro} substitutions were detected. However, virus titers were low after passages 6-7. The passaged viruses were also found to form smaller plaques in A549-ACE2 cells (in the absence of NIR), possibly indicating a replication defect. Thus, passage 6 and 7 viruses were plaque-purified and expanded in A549-ACE2 cells (in the absence of NIR) and sequenced. The number of plaques analyzed was not indicated. The plaque-purified viruses were found to contain M^{pro} F140L+A173V substitutions. It is unclear why the F140L substitution was only detected in plaque-purified viruses.

Table 4. Sequencing of SARS-CoV-2 passaged in the presence of NIR in A549-ACE2 cells.

Passage	NIR (nM)	EC_{50} Multiples	Sample Description	M^{pro} Substitutions ≥50% (Frequency)
1	300	6×	Pooled Sample	none
2	300	6×	Pooled Sample	none
3	1,250	25×	Pooled Sample	A173V (96%)
4	1,250	25×	Pooled Sample	A173V (96%)
	2,000	40×	Pooled Sample	A173V (94%)
5	2,000	40×	Pooled Sample	A173V (93%)
	2,500	50×	Pooled Sample	A173V (88%)
6	2,000	40×	Pooled Sample	A173V (86%)
			Plaque-Purified	F140L (99%)+A173V (97%)
	2,500	50×	Pooled Sample	A173V (71%)
			Plaque-Purified	F140L (99%)+A173V (96%)
7	2,000	40×	Pooled Sample	A173V (85%)
			Plaque-Purified	F140L (98%)+A173V (96%)
	2,500	50×	Pooled Sample	A173V (65%)
			Plaque-Purified	F140L (99%)+A173V (98%)

Source: Adapted from Report 065112, p. 16.

The activity of NIR against two passaged viruses was determined in Vero E6-TMPRSS2 cells by qRT-PCR assay. These experiments were performed in the presence of 2,000 nM CP-100356 (P-gp inhibitor). NIR inhibited replication of the parental virus (SARS-CoV-2 WA1/2020) with a geomean EC_{50} value of 61 nM (Table 5). NIR had similar activity against the P5 virus with the A173V substitution, indicating that the A173V substitution alone may not confer significant NIR resistance, as reported by others (Iketani et al., 2022). However, NIR had significantly reduced activity against the P7 virus with F140L+A173V substitutions, with a 10.1-fold higher EC_{50} value (Table 5). This virus remained fully susceptible to remdesivir.

Table 5. Activity of NIR against SARS-CoV-2 with M^{pro} substitutions.

		EC_{50} (nM)			EC_{90} (nM)		
Virus (M^{pro} Substitutions)	N	Geomean	Fold-Change	p-value	Geomean	Fold-Change	p-value
control (none)	3	61	N/A	N/A	327	N/A	N/A
P5 (A173V)	3	57	0.9	0.88	130	0.4	0.006
P7 (F140L+A173V)	3	614	10.1	<0.001	1,308	4.0	<0.001

Source: Adapted from Report 065112, p. 17. P-values were determined by Dunnett t-test.
N/A, not applicable.

Both the M^{pro} F140L and A173V substitutions have been associated with NIR resistance in cell culture, usually in combination with other M^{pro} substitutions, by independent groups (Iketani et al., 2022; Zhou et al., 2022). However, the F140L+A173V double substitution has not been observed by others. These studies had several limitations. The findings were not confirmed with biochemical assays and recombinant viruses. The sponsor did not indicate whether any of the selected viruses had substitutions in any M^{pro} cleavage sites. Replication kinetics in the absence of NIR were not determined. Alternative resistance pathways may have been missed, as a single virus stock was used to initiate the infections. No data were provided regarding the structural or mechanistic basis of resistance.

"In Vitro Virus RNA Replication Efficiency of the Recombinant SARS-CoV-2 Containing Engineered Mutations (sic) in Mpro" (Report 024518)

To determine the impact of M^{pro} substitutions on NIR activity in cell culture, the sponsor generated recombinant SARS-CoV-2 (WA1/2020-based) viruses using a previously described system (Xie et al., 2020). The sponsor attempted to generate viruses with M^{pro} G15S, Y54A, E55L, E55L+S144A, L89F, K90R, F140A, S144A/E/L/P/T, H164N, E166A/V, H172Y, and Q189K substitutions. The E166V substitution was chosen because it was identified in several NIR-treated participants in trial EPIC-HR. The L89F and K90R substitutions were chosen because they represent naturally occurring polymorphisms that were not expected to affect NIR activity. The other substitutions were chosen because they significantly affected NIR activity in a biochemical assay and/or were identified in NIR-selected mouse hepatitis virus (MHV). These substitutions were chosen prior to completion of the sponsor's studies on NIR-selected SARS-CoV-2 in cell culture and the release of similar studies by independent groups. Of these substitutions, only S144A, E166A/V, and H172Y have been associated with SARS-CoV-2 resistance to NIR in cell culture (Iketani et al., 2022; Jochmans et al., 2022; Zhou et al., 2022).

The sponsor successfully generated 9/17 recombinant viruses with M^{pro} substitutions, while 8/17 viruses could not be generated because: 1) no virus could be recovered, or 2) the virus recovered did not have the expected M^{pro} substitution (Table 6). In 2 cases (H164N and E166A), the initial virus recovered contained a mixture of sequences, but virus with only the desired substitution was obtained by plaque purification. All virus stocks, whether from bulk passaging or plaque purification, were analyzed by Illumina sequencing to confirm the presence of the desired substitutions.

The activity of NIR against recombinant SARS-CoV-2 viruses was tested in Vero E6 P-gp knockout cells by qRT-PCR assay. Cells were infected at an MOI of 0.04 in the presence of NIR and incubated for 48 hours, followed by in-plate lysis and qRT-PCR. NIR inhibited the replication of wild-type (WT) SARS-CoV-2 with a mean EC_{50} value of 37 nM (Table 6). Of the 9/17 viruses successfully generated, only the virus with the E166A substitution had significantly reduced susceptibility to NIR, with an ~3.3-fold higher EC_{50} value. The virus with the S144A substitution had a 2.5-fold higher EC_{50} value, although the difference was not statistically significant. The S144A and E166A substitutions led to 92- and 33-fold reduced NIR activity in a biochemical assay, respectively. It is unclear why the Q189K substitution did not affect NIR activity in cell culture, despite leading to 65-fold reduced NIR activity in a biochemical assay.

Table 6. Activity of NIR against recombinant SARS-CoV-2 with M^{pro} substitutions.

		EC_{50} (nM)			EC_{90} (nM)		
Virus	**n**	**Mean**	**Fold-Change**	**p-value**	**Mean**	**Fold-Change**	**p-value**
WT	18	37	N/A	N/A	100	N/A	N/A
G15S	3	26	0.7	0.97	64	0.6	0.91
Y54A	*ND*						
E55L	4	66	1.8	0.59	133	1.3	0.99
E55L+S144A	*In Progress*						
L89F	3	48	1.3	1.00	212	2.1	0.41
K90R	3	56	1.5	0.94	113	1.1	1.00
F140A	*ND*						

S144A	4	94	2.5	0.08	195	1.9	0.41
S144E	*ND*						
S144L	*ND*						
S144P	*ND*						
S144T	*ND*						
H164N	3	71	1.9	0.58	158	1.6	0.91
E166A	5	122	3.3	0.004	535	5.3	<0.001
E166V	*ND*						
H172Y	*ND*						
Q189K	4	8	0.2	<0.001	24	0.2	0.002

Source: Adapted from Report 024518, p. 24. Details of statistical testing for determination of p-values not provided.
n, number of experiments; N/A, not applicable; ND, no data (viruses could not be recovered); WT, wild-type.

In an independent study, NIR had a 2.2-fold higher EC_{50} value against recombinant SARS-CoV-2 with the M^{pro} S144A substitution, similar to the 2.5-fold change observed by the sponsor (Iketani et al., 2022). Thus, the S144A substitution alone confers only slightly reduced susceptibility to NIR. In two other reports, recombinant SARS-CoV-2 with the M^{pro} E166V substitution was successfully generated and found to have significantly reduced susceptibility to NIR (Iketani et al., 2022; Zhou et al., 2022). The main limitation of the sponsor's study is that most of the M^{pro} substitutions (and combinations of substitutions) that were identified in NIR-selected SARS-CoV-2 (by the sponsor and other groups) have not been tested.

Other Studies Related to NIR Resistance in Cell Culture

- In Iketani et al., 2022 (preprint, not peer-reviewed), SARS-CoV-2 was passaged in Vero E6 cells in the presence of NIR. Three cultures were passaged. Culture #1 acquired 5 M^{pro} substitutions (T21I, C160F, A173V, V186A, T304I) and had 28.5-fold reduced susceptibility to NIR (based on EC_{50} value). Culture #2 acquired 4 M^{pro} substitutions (T21I, L50F, A193P, S301P) and had 28.8-fold reduced susceptibility to NIR. Culture #3 acquired 4 M^{pro} substitutions (L50F, F140L, L167F, T304I) and had 55-fold reduced susceptibility to NIR. SARS-CoV-2 was also passaged in Huh7-ACE2 cells in 480 wells, leading to the identification of 53 NIR-resistant cultures. Fourteen M^{pro} substitutions were identified in at least 2 cultures: T21I, L50F, P108S, S144A, E166A/V, T169I, H172Y, A173V, V186A, R188G, P252L, S301P, and T304I. The T21I and L50F substitutions were proposed to act as compensatory substitutions for the E166V substitution.

- In Jochmans et al., 2022 (preprint, not peer-reviewed), SARS-CoV-2 was passaged in Vero E6 cells in the presence of the M^{pro} inhibitor ALG-097161. The passaged virus acquired L50F, E166A, and L167F M^{pro} substitutions and was cross-resistant to NIR, with a 51-fold higher EC_{50} value.

- In Zhou et al., 2022 (preprint, not peer-reviewed), SARS-CoV-2 was passaged in Vero E6 cells in the presence of the hepatitis C virus NS3/4A protease inhibitor boceprevir or NIR. Boceprevir is known to have activity against SARS-CoV-2 M^{pro} (Ma et al., 2020). Two viruses passaged in the presence of boceprevir were found to have reduced susceptibility to NIR (5-6-fold higher EC_{50} values): one with M^{pro} L50F, C160F, A173V, and A191V substitutions and one with M^{pro} L50F and A173V substitutions. SARS-CoV-2 was also passaged in the presence of NIR. One virus passaged in the presence of NIR acquired M^{pro} T21I and T304I substitutions and had 4-6-fold higher EC_{50} values. Another virus passaged in the presence of NIR acquired M^{pro} L50F and E166V substitutions and had 74-163-fold higher EC_{50} values. The L50F substitution was proposed to act as a compensatory substitution for the E166V and A173V substitutions.

- Table 7 contains a list of all SARS-CoV-2 M^{pro} substitutions that were associated with NIR resistance in cell culture, either in the sponsor's studies or the preprints described above. These substitutions were observed in numerous combinations. Refer to the cited studies for lists of all combinations that have been identified to date.

Table 7. SARS-CoV-2 M^{pro} substitutions associated with NIR resistance in cell culture across different studies (FDA analysis).

M^{pro} Substitution	Contact?[a]	Biochemical Assay K_i Fold-Change	Sponsor's Selection Studies	Iketani 2022	Jochmans 2022	Zhou 2022
T21I	No	1.5	X	X		X
L50F	No	0.2	X	X	X	X
P108S	No	2.8		X		
T135I	No	3.2	X			
F140L	Yes	5.4	X	X		
S144A	Yes	92.0	X	X		
C160F	No	ND		X		X
E166A/V	Yes	33.0/ND		X	X	X
L167F	Yes	ND		X	X	
T169I	No	ND		X		
H172Y	Yes	230		X		
A173V	No	26.0	X	X		X
V186A	Yes	ND		X		
R188G	Yes	ND		X		
A191V	Yes	<1.3	X			X
A193P	No	ND		X		
P252L	No	<0.8		X		
S301P*	No	ND*		X		
T304I*	No	0.9*	X	X		X

a. This column indicates residues in direct contact or close proximity (<5 Å) with NIR based on the sponsor's co-crystal structural analysis.
* Note that S301P and T304I overlap the P6 and P3 positions, respectively, of the nsp5/nsp6 cleavage site located at the C-terminus of M^{pro}.
Yellow highlighting indicates substitutions that were observed in at least 2 studies. Biochemical data are from Report 121015. For Iketani 2022, M^{pro} substitutions associated with NIR resistance in Huh7-ACE2 cells are only listed if they were observed in ≥2 cultures. ND, no data.

FACT SHEET RECOMMENDATIONS

The final virology-related changes to the PAXLOVID™ Fact Sheet for Healthcare Providers agreed to by the sponsor and the FDA are shown below in track changes.

12.4 Microbiology

Antiviral Activity

Nirmatrelvir exhibited antiviral activity against SARS-CoV-2 (USA-WA1/2020 isolate) infection of differentiated normal human bronchial epithelial (dNHBE) cells with EC_{50} and EC_{90} values of 62 nM and 181 nM, respectively, after 3 days of drug exposure.

Nirmatrelvir had similar cell culture antiviral activity (EC_{50} values ≤3-fold relative to USA-WA1/2020) against SARS-CoV-2 isolates belonging to the Alpha (B.1.1.7), Gamma (P.1), Delta (B.1.617.2), Lambda (C.37), Mu (B.1.621), and Omicron (B.1.1.529/BA.1, BA.2, BA.2.12.1, and BA.4) variants. The Beta (B.1.351) variant was the least susceptible tested variant with approximately 3.7-fold reduced susceptibility relative to the USA-WA1/2020 isolate.

Antiviral Activity Against SARS-CoV-2 in Animal Models

Nirmatrelvir showed antiviral activity in BALB/c and 129 mice infected with mouse-adapted SARS-CoV-2. Oral administration of nirmatrelvir at 300 mg/kg or 1,000 mg/kg twice daily initiated 4 hours post-inoculation or 1,000 mg/kg twice daily initiated 12 hours post-inoculation resulted in

reduction of lung viral titers and ameliorated indicators of disease (weight loss and lung pathology) compared to placebo-treated animals.

In addition, the antiviral activities of nirmatrelvir alone (300 mg/kg twice daily), ritonavir alone (50 mg/kg twice daily), and nirmatrelvir combined with ritonavir (300 mg/kg+50 mg/kg twice daily) were evaluated in BALB/c mice infected with mouse-adapted SARS-CoV-2. Dosing was initiated 4 hours post-inoculation. Ritonavir alone did not affect lung viral titers or lung pathology. However, the combination of nirmatrelvir and ritonavir resulted in reduction of lung virus titers and lung pathology relative to nirmatrelvir alone.

Antiviral Resistance in Cell Culture and Biochemical Assays

~~Phenotypic assessments were conducted to characterize the impact of naturally occurring SARS-CoV-2 Mpro polymorphisms on the activity of nirmatrelvir in a biochemical assay using recombinant Mpro enzyme. The clinical significance of these polymorphisms is unknown, and it is also unknown if results from the biochemical assay are predictive of antiviral activity in cell culture. The following Mpro amino acid substitutions were associated with reduced nirmatrelvir activity (≥3-fold higher Ki values): G15S (4.4 fold), T135I (3.5 fold), S144A (91.9 fold), H164N (6.4 fold), H172Y (233 fold), Q189K (65.4 fold), and D248E (3.7 fold). G15S is present in the Lambda variant, which did not have reduced susceptibility to nirmatrelvir (relative to USA-WA1/2020) in cell culture.~~

~~In addition, three SARS-CoV-2 Mpro amino acid positions where polymorphisms have not been naturally observed were evaluated by substituting alanine at these positions and assessing their impact on activity in biochemical assays. These Mpro amino acid substitutions were associated with reduced nirmatrelvir activity (i.e., higher Ki values): Y54A (23.6 fold), F140A (39.0 fold), and E166A (33.4 fold). The clinical significance of substitutions at these Mpro positions is unknown.~~

~~Cell culture resistance selection studies with nirmatrelvir using mouse hepatitis virus (MHV, a betacoronavirus used as a surrogate) resulted in the emergence of Mpro amino acid substitutions: P15A, T50K, P55L, F126L, T129M, and/or S144A. The presence of the substitutions P55L and S144A in MHV Mpro was associated with reduced nirmatrelvir susceptibility (~4 to 5-fold higher EC50 values). These positions correspond to E55 and S144 in SARS-CoV-2 Mpro, respectively. E55L alone did not affect nirmatrelvir activity against SARS-CoV-2 Mpro in a biochemical assay, while S144A reduced nirmatrelvir activity by 91.9 fold (based on Ki value). The clinical relevance of these changes is not known.~~

SARS-CoV-2 M^{pro} residues potentially associated with nirmatrelvir resistance have been identified using a variety of methods, including SARS-CoV-2 resistance selection, testing of recombinant SARS-CoV-2 viruses with M^{pro} substitutions, and biochemical assays with recombinant SARS-CoV-2 M^{pro} containing amino acid substitutions. Table 8 indicates M^{pro} substitutions and combinations of M^{pro} substitutions that have been observed in nirmatrelvir-selected SARS-CoV-2 in cell culture. Individual M^{pro} substitutions are listed regardless of whether they occurred alone or in combination with other M^{pro} substitutions. Note that the M^{pro} S301P and T304I substitutions overlap the P6 and P3 positions of the nsp5/nsp6 cleavage site located at the C-terminus of M^{pro}. Substitutions at other M^{pro} cleavage sites have not been associated with nirmatrelvir resistance in cell culture. The clinical significance of these substitutions is unknown.

Table 8: SARS-CoV-2 M^{pro} Amino Acid Substitutions Selected by Nirmatrelvir in Cell Culture

Single Substitution (EC_{50} value fold change)	T21I (1.1-4.6), L50F (1.4-4.2), P108S (ND), T135I (ND), F140L (ND), S144A (2.2-2.5), C160F (ND), E166A (3.3), E166V (25-267), L167F (ND), T169I (ND), H172Y (ND), A173V (0.9-2.3), V186A (ND), R188G (ND), A191V (ND), A193P (ND), P252L (5.9), S301P (ND), and T304I (2.1-5.5).
≥2 Substitutions (EC_{50} value fold change)	T21I+S144A (9.4), T21I+E166V (83), T21I+A173V (3.1), T21I+T304I (3.0-7.9), L50F+E166V (34-163), L50F+T304I (5.9), T135I+T304I (3.8), F140L+A173V (10.1), H172Y+P252L (ND), A173V+T304I (20.2), T21I+L50F+A193P+S301P (28.8), T21I+S144A+T304I (27.8), T21I+C160F+A173V+V186A+T304I (28.5), T21I+A173V+T304I (15), and L50F+F140L+L167F+T304I (54.7).

Abbreviation: ND=no data.

In a biochemical assay using recombinant SARS-CoV-2 M^{pro} containing amino acid substitutions, the following SARS-CoV-2 M^{pro} substitutions led to ≥3-fold reduced activity (fold-change based on K_i values) of nirmatrelvir: G15S (4.4), Y54A (24.0), T135I (3.2), F140A (39.0), F140L (5.4), S144A (92.0), S144E (470), S144T (160), H164N (6.4), E166A (33.0), E166G (16.0), H172Y (230), A173V (26.0), V186G (13.0), Q189K (65.0), Q192L (28.0), Q192P (33.0), and D248E (3.7). The clinical significance of these substitutions is unknown.

Antiviral Resistance in Clinical Trials

Among subjects in clinical trial EPIC-HR with sequence analysis data available at both baseline and a post-dose sample (n=361 nirmatrelvir/ritonavir-treated, n=402 placebo-treated), the following SARS-CoV-2 M^{pro} or M^{pro} cleavage site amino acid changes were detected as treatment-emergent substitutions that were more common in nirmatrelvir/ritonavir-treated subjects relative to placebo-treated subjects (n=number of nirmatrelvir/ritonavir-treated subjects with emergent substitution); M^{pro} substitutions: A7S/T/V (n=3), L30F (n=3), M82I/R (n=3), G109E/R/V (n=3), P132L/S (n=4), C145F/R/Y (n=3), D153H/Y (n=3), E166V (n=3), T196A/K/M/R (n=4), W207L/S/del (n=5), A260D/T/V (n=8), D263E (n=3), A266P/V (n=3), and V297A/F/del (n=3); M^{pro} ORF1ab cleavage site substitutions: Q5324H/R (n=3), A5328P/S (n=6), and T6449I/P (n=3). In one subject with a baseline M^{pro} L50F substitution, the M^{pro} E166V substitution co-occurred with L50F on Day 5 (included in counts above). The M^{pro} E166V and L50F+E166V substitutions have been associated with nirmatrelvir resistance in cell culture (Table 8). None of these substitutions in M^{pro} ~~gene~~ or cleavage ~~regions~~ sites occurred in nirmatrelvir/ritonavir-treated participants who also experienced hospitalization. Thus, the clinical significance of these substitutions is unknown. ~~In a biochemical assay, the P132H/L/S, A260V, and A266V M^{pro} substitutions did not reduce nirmatrelvir activity (K_i fold change ≤1, <1, and ~2, respectively). The potential phenotypic effect on nirmatrelvir susceptibility for the other substitutions is unknown.~~

Viral RNA Rebound

Post-treatment increases in SARS-CoV-2 RNA shedding levels (i.e., viral RNA rebound) in nasopharyngeal samples were observed on Day 10 and/or Day 14 in a subset of PAXLOVID and placebo recipients in EPIC-HR, irrespective of COVID-19 symptoms. The frequency of detection of post-treatment viral RNA rebound varied according to analysis parameters but was generally similar

among PAXLOVID and placebo recipients, regardless of the rebound definition used. A similar or smaller percentage of placebo recipients compared to PAXLOVID recipients had nasopharyngeal viral RNA results < lower limit of quantitation (LLOQ) at all study timepoints in both the treatment and post-treatment periods.

Post-treatment viral RNA rebound was not associated with the primary clinical outcome of COVID-19-related hospitalization or death from any cause through Day 28 following the single 5-day course of PAXLOVID treatment. Post-treatment viral RNA rebound also was not associated with drug resistance as measured by M^{pro} sequencing. The clinical relevance of post-treatment increases in viral RNA following PAXLOVID or placebo treatment is unknown.

Cross-Resistance

Cross-resistance is not expected between nirmatrelvir and anti-SARS-CoV-2 monoclonal antibodies, molnupiravir, or remdesivir based on their different mechanisms of action.

14.1 Efficacy in Subjects at High Risk of Progressing to Severe COVID-19 Illness

A total of 2,246 subjects were randomized to receive either PAXLOVID or placebo. At baseline, mean age was 46 years; 51% were male; 72% were White, 5% were Black, and 14% were Asian; 45% were Hispanic or Latino; 66% of subjects had onset of symptoms ≤3 days from initiation of study treatment; 47% of subjects were serological negative at baseline; the mean (SD) baseline viral RNA shedding in nasopharyngeal samples~~load~~ was 4.63 $\log_{10}$ copies/mL (2.87); 26% of subjects had a baseline viral RNA shedding~~load~~ of >~~10^~~7 $\log_{10}$ copies/mL~~(units)~~; 6% of subjects either received or were expected to receive COVID-19 therapeutic monoclonal antibody treatment at the time of randomization and were excluded from the mITT and mITT1 analyses.

Jonathan Rawson, Ph.D.
Clinical Virology Reviewer

Patrick R. Harrington, Ph.D.
Clinical Virology Reviewer

CONCURRENCES

Date: _____

DAV/Clin Virol TL/J O'Rear

cc: DAV/RPM/Moruf

This is a representation of an electronic record that was signed electronically. Following this are manifestations of any and all electronic signatures for this electronic record.

/s/

JONATHAN M RAWSON
09/26/2022 09:24:27 AM

PATRICK R HARRINGTON
09/26/2022 09:27:09 AM

JULIAN J O REAR
09/26/2022 01:14:41 PM